

# Probing multipartite entanglement in a coupled Jaynes-Cummings system

Peng Xue,<sup>1,2</sup> Zbigniew Ficek,<sup>3</sup> and Barry C. Sanders<sup>2</sup>

<sup>1</sup>*Department of Physics, Southeast University, Nanjing 211189, People's Republic of China*

<sup>2</sup>*Institute for Quantum Information Science, University of Calgary, Alberta T2N 1N4, Canada*

<sup>3</sup>*The National Centre for Mathematics and Physics, KACST, P.O. Box 6086, Riyadh 11442, Saudi Arabia*

(Received 13 April 2012; published 16 October 2012)

We show how to probe multipartite entanglement in  $N$  coupled Jaynes-Cummings cells where the degrees of freedom are the electronic energies of each of the  $N$  atoms in separate single-mode cavities plus the  $N$  single-mode fields themselves. Specifically we propose probing the combined system as though it is a dielectric medium. The spectral properties and transition rates directly reveal multipartite entanglement signatures. It is found that the Hilbert space of the  $N$  cell system can be confined to the totally symmetric subspace of two states only that are maximally entangled  $W$  states with  $2N$  degrees of freedom.

DOI: [10.1103/PhysRevA.86.043826](https://doi.org/10.1103/PhysRevA.86.043826)

PACS number(s): 42.50.Pq, 03.67.Bg, 42.50.Dv, 75.10.Jm

## I. INTRODUCTION

A single two-level atom coupled to a single cavity, or resonator, mode has been studied intensively since the introduction of the ‘‘Jaynes-Cummings (JC) Model’’ independently by Jaynes and Cummings [1] and by Paul [2] in 1963. Quantum-field effects such as periodic spontaneous collapse and revival [3] are now studied and observed in many systems and as a multitude of manifestations [4]. Coupled JC systems have been proposed as a basis for quantum networks [5] and could behave as a novel condensed-matter system if enough JC systems can be coupled together [6].

In a preliminary study we developed theoretical tools for calculating the spectrum, stationary states, and dielectric susceptibility [7]. Here we use and extend those tools, especially to include the nontrivial open-system effects of spontaneous emission and cavity losses. In particular, we consider the problem of how to probe and characterize such systems experimentally. Two quite different approaches are evident. One approach is to probe each component in a microscopic paradigm, namely, drive and detect the various atoms and cavity modes. Another approach, which we favor, is to treat the coupled JC system as a ‘‘black-box’’ model and probe it as a single unit following a macroscopic paradigm.

Our concept is to regard the coupled JC system as a dielectric medium whose susceptibility carries a signature of the peculiarities of the coupled JC system. Diagonalizing the Hamiltonian of the coupled JC system, we find entangled states and their energies. Using the Fermi’s golden rule, we calculate the transition rates between different manifolds of the energy states of the system. In this paper, we restrict the calculation to transitions from the single-excitation states to the ground state of the system. In particular we show that the dielectric susceptibility of the coupled JC medium reveals, by probe-field spectroscopy, quadripartite entanglement of the system comprising mutually coupled atoms and cavity modes. Based on our theoretical framework for JC systems mutually coupled by overlapping extra-cavity longitudinal fields, we can calculate stationary states for the coupled system, energy spectrum, and dielectric susceptibility.

The paper is organized as follows. In Sec. II we give a qualitative discussion and a detailed calculation of radiative properties of a single JC cell. Section III is devoted to

the discussion of the entangled and radiative properties of two coupled JC cells. We derive single-excitation states of the system and show that they are the  $W$  state class corresponding to a superposition state of single excitations amongst each of the two atoms and two modes. We then find under which conditions the states reduce to the maximally entangled four-qubit  $W$  states, and how to quantify the degree of entanglement of the states using probe-field spectroscopy methods. A generalization of the calculation to an arbitrary number of mutually coupled JC cells is presented in Sec. IV. Finally, in Sec. V, we summarize our results.

## II. ENTANGLEMENT AND RADIATIVE PROPERTIES OF THE SINGLE JC CELL

The JC cell (as we refer to a single JC system) is a composite atom cavity-mode system that radiates via two distinct channels. The closed coupled JC system is characterized by just two parameters, namely, the atom-cavity coupling rate  $g$  and the intercavity coherent hopping rate  $\kappa$ . One radiative channel arises due to coupling of the atom to the cavity side modes (free-space modes) causing spontaneous decay of the atomic excitation with an inhibited spontaneous emission rate  $\gamma_a$ . The inhibition refers to the fact that some free radiative modes are suppressed by cavity confinement of the atom. The other radiative decay mode is due to losses from one or both mirrors of the optical cavity at rate  $\gamma_c$ . We assume independence between these two radiative channels.

A single JC cell comprises a single cavity field mode of frequency  $\omega_c$  and a two-level atom with energy states  $|g_i\rangle$  and  $|e_i\rangle$  and corresponding energy difference

$$\hbar\omega_a = E_e - E_g. \quad (1)$$

The atom is coupled to the cavity mode with coupling constant  $g$ , which we choose to be real with no loss of generality. We assume that the atomic transition frequency is detuned from the cavity frequency by  $\Delta = \omega_a - \omega_c$ .

In the rotating-wave approximation, and using a system of units in which  $\hbar \equiv 1$ , the Hamiltonian of the single JC system is

$$\hat{H}^{\text{JC}} = \omega_c(\hat{a}^\dagger\hat{a} + \frac{1}{2}) + \frac{1}{2}\omega_a\hat{\sigma}_z + g(\hat{a}^\dagger\hat{\sigma}_- + \hat{a}\hat{\sigma}_+), \quad (2)$$

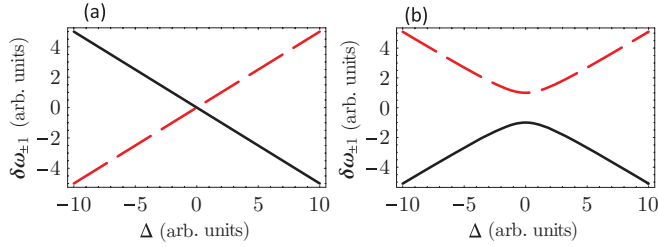


FIG. 1. (Color online) Variation of the energy difference  $\delta\omega_{\pm 1} = \omega_{\pm 1} - \omega_c$  of the  $n = 1$  eigenstates with the detuning  $\Delta$  (in arbitrary units);  $\delta\omega_{-1}$  (black solid line) and  $\delta\omega_{+1}$  (red dashed line) for a single JC cell with (a)  $g = 0$  and (b)  $g = 1$ .

with  $\hat{a}^\dagger$  and  $\hat{a}$  the creation and annihilation operators of the cavity mode, respectively, and  $\hat{\sigma}_\pm$  and  $\hat{\sigma}_z$ , with  $\text{spec}(\hat{\sigma}_z^i) = \pm 1$ , the spin operators for the atom.

### A. Energy spectrum

The JC energy spectrum comprises a ground state of energy  $\omega_0 = -\Delta/2$  and a ladder of doublets of energies

$$\omega_{\pm n} = n\omega_c \pm \sqrt{ng^2 + \frac{1}{4}\Delta^2}, \quad n = 1, 2, \dots \quad (3)$$

The corresponding stationary energy states are the ground state  $|0g\rangle$  and the excited state doublets,

$$\begin{aligned} |+, n\rangle &= \cos \theta_n |e, n-1\rangle + i \sin \theta_n |g, n\rangle, \\ |-, n\rangle &= -\sin \theta_n |e, n-1\rangle + i \cos \theta_n |g, n\rangle, \end{aligned} \quad (4)$$

with

$$2\theta_n = \tan^{-1} \left( \frac{2g\sqrt{n}}{\Delta} \right). \quad (5)$$

Note that the doublets are in a pure, bipartite entangled state of the atom and the field. This entanglement is maximal (for all the doublets) only when  $\Delta = 0$ .

Figure 1 shows a variation of the energies  $\omega_{\pm n}$  of the  $n = 1$  doublet  $|\pm, 1\rangle$  with the detuning  $\Delta$  around the unperturbed energy  $\omega_c$ . Notice the level crossing in the absence of the coupling  $g$  at  $\Delta = 0$ , and the appearance of the familiar avoided crossing effect when  $g \neq 0$ .

In the following we explore the radiative properties of this single JC cell, in particular looking for signatures of this atom-field entanglement in the transition rates between states with different total number of excitations. Specifically, we search for conditions that reveal whether the entanglement of the eigenstates (4) is maximal or not.

### B. Transition rates

As we have seen, each doublet has some fixed number of quanta shared between the atom's electronic state and the cavity-mode field state. We employ the integer  $\nu$  to designate the number of quanta in the system. The ground state corresponds to  $\nu = 0$ , which means that the electronic state and field state are both in the lowest level. The first doublet has  $\nu = 1$  quantum, the second doublet has  $\nu = 2$  quanta, and so on.

Consider first the case  $n = 1$  with transitions from the single-excitation states  $|\pm, 1\rangle$ , with splitting due to the atom-field interaction, to the ground state, which is a product state not affected by the atom-field interaction. The transition rates from the excited states to the ground state are given by Fermi's golden rule [8],

$$\Gamma_{\pm, 1} = \gamma_a |\langle 1, \pm | \hat{\sigma}_+ | g, 0 \rangle|^2 + \gamma_c |\langle 1, \pm | \hat{a}^\dagger | g, 0 \rangle|^2. \quad (6)$$

These transition rates are a sum of transitions caused by spontaneous emission from the atom, with rate  $\gamma_a$ , and by damping of the cavity mode, with rate  $\gamma_c$ . Consequently the coefficient  $\gamma_a$  quantifies the amount that the atomic spontaneous emission contributes to the transition probability. Similarly,  $\gamma_c$  quantifies how much the cavity losses contribute to the transition probability.

From Eq. (4) we readily calculate the transition dipole moments between the states  $|\pm, 1\rangle$  and  $|g, 0\rangle$  whence we obtain the transition probabilities

$$\Gamma_{+, 1} = \gamma_c + (\gamma_a - \gamma_c) \cos^2 \theta_1, \quad \Gamma_{-, 1} = \gamma_a - (\gamma_a - \gamma_c) \cos^2 \theta_1. \quad (7)$$

A number of interesting properties are immediately evident from the expressions for these probabilities. For example, in the absence of either atomic spontaneous emission ( $\gamma_a = 0$ ) or cavity dissipation ( $\gamma_c = 0$ ), that is, when only a single dissipation channel is present in the system, the transition probabilities depend on the nature of the states from which they originate, with this nature given by the parameter  $\theta_1$  as appears in Eqs. (4) and (5).

This dependence on  $\theta_1$  causes the two transition probabilities to be mutually correlated. For example, an increase of  $\Gamma_{+, 1}$  implies a decrease of  $\Gamma_{-, 1}$ , and vice versa. The probabilities become independent of each other and their magnitudes equalize only when the states become maximally entangled. Thus, we may infer from the transition probabilities to what degree the states are entangled. However, this conclusion is based on a simplified model of the system involving only a single decay channel, which is incompatible with what one encounters in practice. A practical JC system radiates through both dissipation channels.

We distinguish here two parameter regimes with a qualitatively different behavior for the transition probabilities. These two regimes are distinguished according to the magnitude of  $\gamma_c$  relative to  $\gamma_a$ . When the dissipation rates are equal,  $\gamma_a = \gamma_c \equiv \gamma$ , Eq. (7) yields that the probabilities are independent of each other and have equal magnitudes,  $\Gamma_{+, 1} = \Gamma_{-, 1} = 2\gamma$ , regardless of the state of the system (i.e.,  $\theta_1$ ). In other words, the transition probabilities tell us nothing about the nature of the states involved. In physical terms, this is a consequence of the fact that, for  $\gamma_a = \gamma_c$ , one cannot distinguish which dissipation channel is used by the quantum leaving the JC system, regardless of the initial state. Therefore, determining the entanglement of the states  $|\pm, 1\rangle$  is not possible from transition rates if  $\gamma_a = \gamma_c$ , so of course the setup must then avoid this condition for entanglement to be measurable.

For  $\gamma_a \neq \gamma_c$ , the transition rates depend explicitly on the amplitudes of the states involved, thereby enabling the degree of entanglement to be discerned from the transition rates, for example, by measuring the difference or the ratio between

$\Gamma_{+,1}$  and  $\Gamma_{-,1}$ . From Eq. (7) we see that, for nonmaximally entangled states ( $\cos^2 \theta_1 \neq 1/2$ ), equality between  $\Gamma_{+,1}$  and  $\Gamma_{-,1}$  cannot be achieved. However, when  $\cos^2 \theta_1 = 1/2$ , which corresponds to the case of maximally entangled states,  $\Gamma_{+,1}$  and  $\Gamma_{-,1}$  have the same magnitude. Equality between the transition probabilities with  $\gamma_a \neq \gamma_c$  can only occur for maximally entangled states.

We now consider the case  $n \geq 2$ . In this case, transitions occur between two neighboring doublets of entangled states ( $n = 2$  and  $n = 1$ ). Notice that the transitions occur between states of different degree of entanglement, and there are two possible transition channels from each state of the upper doublet to states of the doublet below. Transitions from the  $i$ th to the  $j$ th state of the neighboring  $n$  and  $n - 1$  doublets occur with rate

$$\Gamma_{i,jn} = \gamma_a |\langle n, i | \hat{\sigma}^+ | j, n - 1 \rangle|^2 + \gamma_c |\langle n, i | a^\dagger | j, n - 1 \rangle|^2. \quad (8)$$

Using Eqs. (4) and (8), we readily find that the transitions occur with probabilities

$$\begin{aligned} \Gamma_{+,\pm n} &= \frac{1}{2} [(\gamma_a - \gamma_c) \mp (\gamma_a + \gamma_c) \cos 2\theta_{n-1}] \cos^2 \theta_n \\ &\quad + \frac{1}{2} n \gamma_c (1 \pm \cos 2\theta_n \cos 2\theta_{n-1}) \\ &\quad \pm \frac{1}{2} \gamma_c \sqrt{n(n-1)} \sin 2\theta_n \sin 2\theta_{n-1}, \\ \Gamma_{-,\pm n} &= \frac{1}{2} [(\gamma_a - \gamma_c) \mp (\gamma_a + \gamma_c) \cos 2\theta_{n-1}] \sin^2 \theta_n \\ &\quad + \frac{1}{2} n \gamma_c (1 \mp \cos 2\theta_n \cos 2\theta_{n-1}) \\ &\quad \mp \frac{1}{2} \gamma_c \sqrt{n(n-1)} \sin 2\theta_n \sin 2\theta_{n-1}, \end{aligned} \quad (9)$$

thereby yielding

$$\begin{aligned} \Gamma_{+,n} &= \sum_{j=\pm} \Gamma_{+,j,n} = n\gamma_c + (\gamma_a - \gamma_c) \cos^2 \theta_n, \\ \Gamma_{-,n} &= \sum_{j=\pm} \Gamma_{-,j,n} = n\gamma_c + (\gamma_a - \gamma_c) \sin^2 \theta_n, \end{aligned} \quad (10)$$

for the total transition probabilities from the states  $|\pm, n\rangle$ .

Although the transitions occur between states of different degrees of entanglement, the total transition probabilities are determined *only* by the amplitudes of the states of the upper doublet. The states of the lower doublet do not become involved. The properties of the total probabilities are essentially similar to those discussed above for the transitions from the  $n = 1$  doublet to the ground state. Indeed, for  $n = 1$ , the probabilities (10) reduce to Eq. (7), and unequal damping rates,  $\gamma_a \neq \gamma_c$ , ensures the dependence of the transition probabilities on the degree of entanglement.

Thus, transition rates of a combined quantum system depend strongly on how the subsystems decay rather than on the nature of states involved. The presence of the maximally entangled states in a JC cell could be observed in principle by measuring the transition rates between energy levels of the system, subject to  $\gamma_a \neq \gamma_c$ .

### C. Absorption spectrum of a weak probe beam

There remains the question of how these properties of the transition rates might be exhibited experimentally. Probe-beam spectroscopy methods should be able to test these properties. When a JC system is irradiated by a weak probe beam with a frequency that is close to resonance, the rate at which the

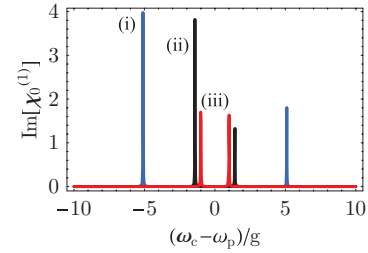


FIG. 2. (Color online) The absorption spectra  $\text{Im}[\chi_0^{(1)}(\omega_p)]$  of a probe beam monitoring a single JC cell for  $\gamma_a/g = 0.05$ ,  $\gamma_c/g = 0.02$ ,  $\gamma/g = 0.01$ , and different detunings:  $\Delta/g = 0$  [red line (iii)],  $\Delta/g = 2$  [black line (ii)], and  $\Delta/g = 10$  [blue line (i)].

probe beam is absorbed is proportional to the transition rates between the energy states of the system.

We consider net absorption by the system of radiation from a tunable beam probing the system. The probe-beam intensity is assumed to be sufficiently weak such that the field is treated to only first order in its amplitude so that it does not appreciably perturb the system. The absorption spectrum is given by the imaginary part of the linear susceptibility  $\chi_0^{(1)}(\omega_p)$  of the system [9–11],

$$\text{Im}[\chi_0^{(1)}(\omega_p)] = \sum_{i,n} \frac{\gamma \Gamma_{i,n}}{(\omega_{in} - \omega_p)^2 + \gamma^2}, \quad (11)$$

where  $\omega_p$  is the frequency of a probe beam,  $\Gamma_{i,n}$  is the total transition rate from the state  $i$  ( $i = \pm$ ) of the manifold  $n$ , and  $\gamma$  describes the width of a given transition. In writing expression (11), we have used the fact that transitions from the excitation states to states of the manifold below might not be purely radiative [8,12], i.e.,  $\gamma \neq \Gamma_{i,n}/2$ , and the system was in the  $n - 1$  manifold before the probe was applied. To ensure that the spectral lines are well resolved, we assume that the transitions do not overlap. This is achieved assuming that the coupling strength  $g$  is much larger than the transition rates  $\Gamma_{i,n}$ .

Figure 2 shows absorption spectra of a probe beam tuned in the vicinity of the transition frequencies from the  $n = 1$  doublet to the ground state of a single JC cell. We see that as long as  $\Delta \neq 0$ , the spectrum of the single cell is markedly asymmetric. This feature is associated with the fact that at  $\Delta \neq 0$ , the transitions from the  $n = 1$  doublet to the ground state occur with different rates,  $\Gamma_{+,1} \neq \Gamma_{-,1}$ . The spectrum becomes symmetric at resonance, where  $\Delta = 0$ . The symmetric spectrum is associated with the fact that at the resonance,  $\Gamma_{+,1} = \Gamma_{-,1}$ . As predicted by Eq. (7), the equality of the total transition rates takes place only for the maximally entangled states. Therefore, the symmetry of the spectrum can be regarded as an indication of the presence of maximally entangled states.

### III. TWO MUTUALLY COUPLED JC CELLS

We now consider two neighboring JC cells coupled via overlapping evanescent waves of the cavity modes. The coupling results in a coherent hopping rate  $\kappa$  between cavities. We designate  $\hat{a}_i$  and  $\hat{\sigma}_i$  as the field annihilation operator and atomic electron energy lowering operator for the  $i$ th JC cell,

and the double JC cell Hamiltonian is [7,13–16]

$$\hat{H} = \hat{H}_1^{\text{JC}} + \hat{H}_2^{\text{JC}} - \kappa(\hat{a}_1^\dagger \hat{a}_2 + \hat{a}_1 \hat{a}_2^\dagger) = \bigoplus_{\nu} \hat{H}^{(\nu)}, \quad (12)$$

with  $\nu$  denoting the total number of quanta shared in the two-cavity system.

The space of the system for any  $\nu$  is spanned by product states  $\{|n_1, c_1, n_2, c_2\rangle\}$  with  $n_i$  a label for the number of photons in the  $i$ th cavity and  $c_i$  the label for whether the state is in the excited ( $|e\rangle$ ) or ground ( $|g\rangle$ ) state. For example, the ground state corresponds to  $\nu = 0$  with just one dimension and hence contains one basis element  $\{|0g0g\rangle\}$ . The single-excitation ( $\nu = 1$ ) basis comprises four states  $\{|0e0g\rangle, |1g0g\rangle, |0g1g\rangle, |0g0e\rangle\}$ .

In the following, we limit ourselves to the subspace  $\nu = 1$  that only a single excitation is present in the system. The  $\nu = 1$  case is especially interesting as it corresponds to four qubits: two two-level atoms and two field modes with superpositions of vacuum and single-photon states. Also the  $\nu = 1$  case can be solved in closed form yielding simple expressions [7].

### A. Entangled four-qubit states

A diagonalization of the Hamiltonians  $\hat{H}^{(\nu)}$  for  $\nu = 0, 1$  yields the energy spectra  $\omega^{(0)} = -\Delta$  for the ground state, and

$$\omega_{\epsilon\epsilon}^{(1)} = \omega_c - \frac{1}{2}(\Delta + \epsilon\kappa) + \epsilon\sqrt{g^2 + \frac{1}{4}(\Delta + \epsilon\kappa)^2} \quad (13)$$

for the single excitation, with  $\epsilon = \pm$  and  $\epsilon = \pm$ . In the case of independent cells,  $\kappa = 0$ , and then the upper spectral value is degenerate,

$$\omega_{\epsilon\epsilon}^{(1)}|_{\kappa=0} = \omega^{\text{JC}(0)} + \omega_e^{\text{JC}(1)}, \quad (14)$$

and the spectrum corresponds to what is expected for two independent JC systems, with  $\epsilon$  being irrelevant.

On the other hand, for  $g = 0 = \Delta$ , the  $\nu = 0$  spectrum is characterized by  $\omega^{(0)} = 0$ , whereas the  $\nu = 1$  is described by  $\omega_{\epsilon\epsilon}^{(1)}|_{g=0=\Delta}$ , which is the doubly-degenerate  $\omega_c$  or  $\omega_c + \epsilon\kappa$  values as expected for coupled harmonic oscillators. Therefore, a large intercavity hopping rate will push the coupled JC cells to behaving closely like coupled harmonic oscillators with atom-cavity perturbations. For small  $\kappa$ ,

$$\omega_{\epsilon\epsilon}^{(1)} \approx \omega_c + \epsilon g - \frac{\epsilon\kappa}{2} + \epsilon \frac{\kappa^2}{8g}, \quad (15)$$

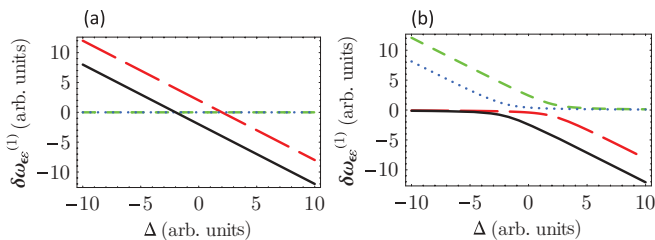


FIG. 3. (Color online) The dependence of the energy difference  $\delta\omega_{\epsilon\epsilon}^{(1)} = \omega_{\epsilon\epsilon}^{(1)} - \omega_c$  on the detuning  $\Delta$  (in arbitrary units) of the  $\nu = 1$  states,  $|+, -\rangle$  (black solid line),  $|-, -\rangle$  (red long-dashed line),  $|-, +\rangle$  (green short-dashed line),  $|+, +\rangle$  (blue dotted line), for two coupled JC cells with (a)  $g = 0, \kappa = 2$  and (b)  $g = 1, \kappa = 2$ .

with shift  $\pm g$  due to vacuum Rabi splitting,  $\epsilon\kappa/2$  the normal-mode splitting due to intercavity coupling, and  $\epsilon\kappa^2/8g$  a frequency pulling effect similar to the ac Stark shift.

Figure 3 shows the variation of the energies  $\omega_{\epsilon\epsilon}^{(1)}$  of the single excitation  $\nu = 1$  states with the detuning  $\Delta$  around the unperturbed energy  $\omega_c$ . In the absence of the coupling  $g$ , there are two crossing points at  $\Delta = \pm\kappa$ . The coupling lifts the degeneracy resulting in four entangled states. The states are eigenstates of the Hamiltonian (12) corresponding to the energies  $\omega_{\epsilon\epsilon}^{(1)}$ , and are of the form [7]

$$|\epsilon, \epsilon\rangle = u_{\epsilon, \epsilon}(|1g0g\rangle - \epsilon|0g1g\rangle) + w_{\epsilon, \epsilon}(|0e0g\rangle - \epsilon|0g0e\rangle), \quad (16)$$

where

$$u_{\epsilon, \epsilon} = \frac{-r_\epsilon + \epsilon\sqrt{1+r_\epsilon^2}}{\sqrt{2+2(r_\epsilon - \epsilon\sqrt{1+r_\epsilon^2})^2}}, \quad (17)$$

$$w_{\epsilon, \epsilon} = \frac{1}{\sqrt{2+2(r_\epsilon - \epsilon\sqrt{1+r_\epsilon^2})^2}},$$

and

$$r_\epsilon = (\Delta + \epsilon\kappa)/(2g). \quad (18)$$

The double JC states (16) are in the  $W$  state class corresponding to a superposition state of single excitations amongst each of the two atoms and two modes. These states are maximally entangled only for  $u_{\epsilon, \epsilon} = w_{\epsilon, \epsilon} = 1/2$ , which requires that  $r_\epsilon = 0$ . The condition that  $r_\epsilon = 0$  is met only if  $\Delta = \epsilon\kappa$ . Radiative properties of two coupled JC cells are studied in the next section.

### B. Transition rates and their collective properties

We can compute the transition probabilities [17–19]

$$\Gamma_{\epsilon, \epsilon} = \gamma_a |\langle \epsilon, \epsilon | (\hat{\sigma}_1^+ + \hat{\sigma}_2^+) | 0 \rangle|^2 + \gamma_c |\langle \epsilon, \epsilon | (a_1^\dagger + a_2^\dagger) | 0 \rangle|^2 \quad (19)$$

from the single-excitation states  $|\epsilon, \epsilon\rangle$  to the ground state  $|0g0g\rangle \equiv |0\rangle$ , which yields

$$\Gamma_{\epsilon, \epsilon} = (1 - \epsilon)^2 (\gamma_a |w_{\epsilon, \epsilon}|^2 + \gamma_c |u_{\epsilon, \epsilon}|^2). \quad (20)$$

The dependence of the transition rates on  $\epsilon$  signals the existence of superradiant ( $\epsilon = -$ ) and metastable nonradiative ( $\epsilon = +$ ) states in the system [20,21]. Note that the equality of the superradiant rates,  $\Gamma_{-,+} = \Gamma_{-,-}$ , is a signature of the maximal entanglement present in the corresponding states. However, this signature is not present for the other two states  $|+, \epsilon\rangle$ , as these do not imprint a signature on the radiation properties of the system.

Notice that these collective radiative properties of the system are independent of the ratio  $\gamma_a/\gamma_c$  and of the nature of the states. These decay processes are due to losses of the coupled cavity modes as well as by atomic spontaneous emission. This latter feature is surprising because atoms are not directly coupled to each other, and they behave independent of the ratio  $\kappa/g$ . The existence of the metastable states implies that the double JC system effectively behaves as a single collective JC cell composed of a doublet consisting of four-qubit entangled states  $|\epsilon, -\rangle$ .

The metastable states could be made radiatively active by breaking the symmetry between the atoms and/or the cavity modes of *different* JC cells, for example, by allowing the atoms and the cavity modes to decay at different rates. It is easy to show that when the atoms are damped with different rates, say  $\gamma_{a1}$  and  $\gamma_{a2}$ , and the cavity losses occur with rates  $\gamma_{c1}$  and  $\gamma_{c2}$ , respectively, then the transitions from the states  $|\epsilon, \epsilon\rangle$  occur with probabilities

$$\Gamma_{\epsilon, \epsilon} = (\sqrt{\gamma_{a1}} - \epsilon\sqrt{\gamma_{a2}})^2 |w_{\epsilon, \epsilon}|^2 + (\sqrt{\gamma_{c1}} - \epsilon\sqrt{\gamma_{c2}})^2 |u_{\epsilon, \epsilon}|^2. \quad (21)$$

Clearly, the transition probabilities are different from zero, irrespective of  $\epsilon$ . However, the states retain their collective character with the  $\epsilon = -$  states still behaving as a superradiant and the  $\epsilon = +$  states now behaving as a subradiant state.

There are some similarities in the properties of the transition probabilities of the double and single JC cell systems, in particular, when the atomic spontaneous emission and cavity losses in a JC cell occur with the same rate. For example, in the case of  $\gamma_{a1} = \gamma_{c1}$  and  $\gamma_{a2} = \gamma_{c2}$ , the probabilities (21) become independent of the amplitudes of the states, which is the same property encountered for  $\Gamma_{\pm 1}$  of the single cell.

However, there are interesting differences. In the double JC system, the condition  $\gamma_{ai} \neq \gamma_{ci}$  is necessary but not sufficient for the dependence of the transition rates on the amplitudes of the states. There is also a rather subtle condition of the relation between the damping rates of different cells to be satisfied. Even though the spontaneous emission and cavity losses in a given JC cell occur with different rates,  $\gamma_{ai} \neq \gamma_{ci}$ , the transition probabilities still could be independent of the amplitudes of the states. This happens when  $\gamma_{a1} = \gamma_{c2}$  and  $\gamma_{a2} = \gamma_{c1}$ , for which Eq. (21) reduces to

$$\Gamma_{\epsilon, \epsilon} = \frac{1}{2}(\sqrt{\gamma_{a1}} - \epsilon\sqrt{\gamma_{c1}})^2. \quad (22)$$

Evidently, the transition rates are independent of the amplitudes of the states. The quantitative reason for this is that, even if the cells are distinguished by different damping rates, they are directly coupled to each other through the coupling  $\kappa$ . This coupling creates entangled states between the cells that in the case of  $\gamma_{a1} = \gamma_{c2}$  make indistinguishable through which channel,  $\gamma_{a1}$  or  $\gamma_{c2}$ , a photon leaving the system was emitted. This property is characteristic of multicell JC systems and does not exist in a single JC cell. Therefore, under the condition that all the damping rates are different, equality between the superradiant (subradiant) rates signals maximal entanglement in the superradiant (subradiant) states,  $|-, \epsilon\rangle$  ( $|+, \epsilon\rangle$ ), which generalizes the results of the single JC cell.

### C. Absorption spectra

We now consider absorption spectra of a weak radiation monitoring the transitions from the single-excitation ( $\nu = 1$ ) states to the ground state  $|0\rangle$  of two identical JC cells. To ensure that the probe field couples exclusively to the single-excitation states, we assume that the transitions do not overlap. This is achieved assuming that the coupling strengths  $g$  and  $\kappa$  are much larger than the transition rates  $\Gamma_m$ .

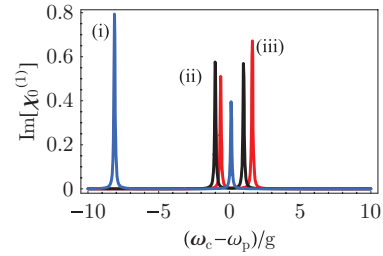


FIG. 4. (Color online) The absorption spectra  $\text{Im}[\chi_0^{(1)}(\omega_p)]$  of a probe beam monitoring two coupled identical JC cells, for  $\gamma_a/g = 0.05$ ,  $\gamma_c/g = 0.02$ ,  $\gamma/g = 0.01$ ,  $\kappa/g = 2$ , and different detunings:  $\Delta/g = 1$  [red line (iii)],  $\Delta/g = 2$  [black line (ii)], and  $\Delta/g = 10$  [blue line (i)].

Figure 4 shows absorption spectra for  $\gamma_a \neq \gamma_c$  and different detunings  $\Delta$ . We see that as long as  $\Delta \neq \pm\kappa$ , the spectrum is always asymmetric. The spectrum becomes symmetric when  $\Delta = \kappa$ . In this case, the states  $|\pm, -\rangle$  are maximally entangled states. Thus, similar to the case of a single JC cell, the symmetry of the spectrum can be regarded as an indication of the presence of maximally entangled states. Note that the symmetric spectrum is observed at nonzero detunings,  $\Delta = \pm\kappa$ , which is in contrast to the properties of the spectrum of a single cell, where the symmetric spectrum is observed only at resonance, where  $\Delta = 0$ .

Figure 5 shows the absorption spectrum for a more general case of unequal damping rates of the atoms ( $\gamma_{a1} \neq \gamma_{a2}$ ) and of the cavity modes ( $\gamma_{c1} \neq \gamma_{c2}$ ). In this case, the spectrum comprises four peaks corresponding to the transition rates of the four eigenstates  $|\epsilon, \epsilon\rangle$ . Two of the peaks are high (corresponding to the superradiant states  $|-, \epsilon\rangle$ ) and two are short (corresponding to the subradiant states  $|+, \epsilon\rangle$ ). According to our predictions, whenever the high (short) peaks have the same height and are located in opposite sides around the cavity frequency, this condition corresponds to a signature of the underlying maximal entanglement of the superradiant (subradiant) states. The joint  $\gamma_{a1} = \gamma_{a2}$  and  $\gamma_{c1} = \gamma_{c2}$  case is special because, in this case, the subradiant states are optically inactive and only the peaks corresponding to the superradiant states are present in the spectrum. Therefore, the symmetry of the spectrum around the cavity frequency increases as the superradiant states  $|-, \epsilon\rangle$  become increasingly entangled. Note that, in order to resolve the peaks, the linewidth of the probe

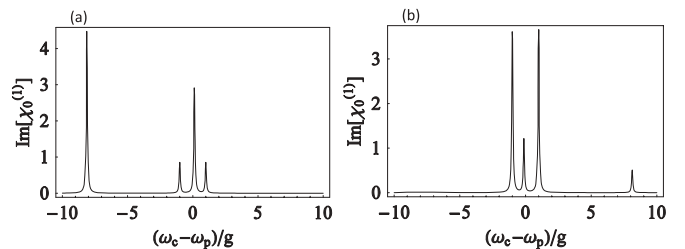


FIG. 5. The absorption spectra  $\text{Im}[\chi_0^{(1)}(\omega_p)]$  of a probe beam monitoring the system of two nonidentical JC cells for  $(\gamma_{a1}/g, \gamma_{a2}/g) = (0.01, 0.2)$ ,  $(\gamma_{c1}/g, \gamma_{c2}/g) = (0.2, 0.05)$ ,  $\kappa/g = 4$ ,  $\gamma/g = 0.05$ , and different  $\Delta$ : (a)  $\Delta/g = -4$  and (b)  $\Delta/g = 4$ .

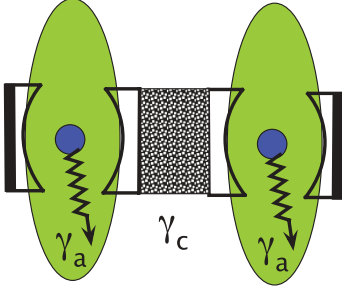


FIG. 6. (Color online) Two distant cells with the cavity modes overlapping in the shadow area. This area can also be treated as a common reservoir for the cavity modes to which the modes are damped with rate  $\gamma_c$ . The atoms located in the distance cavities are damped by independent reservoirs (green areas) with rate  $\gamma_a$ .

beam has to be sufficiently narrow compared with the cavity and atomic damping rates.

#### D. Atoms damped by independent reservoirs

In the above analysis we have assumed that the atoms and the cavity modes are damped by common reservoirs. This assumption is justified if the cells are quite close to each other where the spatial variation of the field can be ignored. This assumption may not always be true in practice as the cells could be separated by a large distance. In this case, the assumptions that the atoms are coupled to the same reservoir might not be true. For this reason, we consider now a situation, illustrated in Fig. 6, in which atoms located in distant cells are damped by independent reservoirs.

In the case of independent reservoirs for the atoms, the transition probabilities from the single-excitation states  $|\epsilon, \epsilon\rangle$  to the ground state  $|0\rangle$  are given by

$$\Gamma_{\epsilon, \epsilon} = \gamma_a (|\langle \epsilon, \epsilon | \hat{\sigma}_1^+ | 0 \rangle|^2 + |\langle \epsilon, \epsilon | \hat{\sigma}_2^+ | 0 \rangle|^2) + \gamma_c |\langle \epsilon, \epsilon | (a_1^\dagger + a_2^\dagger) | 0 \rangle|^2, \quad (23)$$

which yields

$$\Gamma_{\epsilon, \epsilon} = 2\gamma_a |w_{\epsilon, \epsilon}|^2 + (1 - \epsilon)^2 \gamma_c |u_{\epsilon, \epsilon}|^2. \quad (24)$$

We see that, in the case of independent reservoirs for the atoms, the transition probabilities  $\Gamma_{\epsilon, \epsilon}$  all become different from zero. There are no trapping (subradiant) states that would form a subspace of decoherence-free states. However, in the limit of  $|w_{\epsilon, \epsilon}|^2 = 0$ , the states  $\epsilon = +$  would form a decoherence-free subspace.

A close look at Eq. (17) reveals that the amplitudes  $|w_{\epsilon, -}|^2$  vanish in the limit of  $r_\epsilon \gg 1$ . The condition of  $r_\epsilon \gg 1$  is met when  $(\Delta + \epsilon\kappa) \gg g$ , which shows that either the atomic transition frequencies differ significantly from the cavity frequency,  $\Delta \gg 0$ , or the cells are strongly coupled to each other,  $\kappa \gg 0$ . Under this condition,

$$|w_{\epsilon, -}|^2 = |u_{\epsilon, +}|^2 \approx 0, \quad (25)$$

and

$$|w_{\epsilon, +}|^2 = |u_{\epsilon, -}|^2 \approx \frac{1}{2}. \quad (26)$$

As a consequence, the states of the system in Eq. (16) reduce to

$$|\epsilon, +\rangle = \frac{1}{\sqrt{2}}(|eg\rangle - \epsilon|ge\rangle)|00\rangle, \quad (27)$$

$$|\epsilon, -\rangle = \frac{1}{\sqrt{2}}(|10\rangle - \epsilon|01\rangle)|gg\rangle,$$

with the corresponding transition probabilities

$$\Gamma_{\epsilon, +} = \gamma_a, \quad \Gamma_{\epsilon, -} = \frac{1}{2}(1 - \epsilon)^2 \gamma_c. \quad (28)$$

Clearly, the transition probability  $\Gamma_{+, -} = 0$ , so that the state  $|+, -\rangle$  is a decoherence-free state.

We stress that, in contrast to the states (16) damped by a common reservoir, the states (27) are product states with atom-cavity decoupling due to having independent reservoirs and strong intercell coupling. Effectively, the system behaves as a two-qubit system. Our prediction agrees with the results of de Ponte *et al.* [16], who considered a system of coupled resonators interacting with independent reservoirs and found that the resonators must be strongly coupled to each other for the accomplishment of the condition leading to the decoherence-free states.

#### IV. GENERALIZATION TO AN ARBITRARY NUMBER OF COUPLED JC CELLS

Although the focus of this work is on two coupled JC cells, we can solve the problem more generally. In this section we show how to solve elegantly the case of  $N$  mutually connected JC cells with the Hamiltonian

$$\hat{H}_N = \sum_{i=1}^N \hat{H}_{\text{JC}}^i - \kappa \sum_{i \neq j} (\hat{a}_i^\dagger \hat{a}_j + \text{H.c.}). \quad (29)$$

The Hamiltonian describes a system composed of  $N$  identically coupled cells. While this description does not include such features as the direct coupling between the atoms and the spatial variation of the field modes, it is nevertheless of interest, as the simplest model of a group of collective behaving cells. This case is somewhat artificial for large  $N$ , but does yield an instructive generalization of the formalism in addition to providing some connection with condensed-matter studies of coupled JC systems [6].

##### A. Energy spectrum

Restricting to the single excitation,  $\nu = 1$ , the space of the system is spanned by  $2N$  product states

$$\{|0g0g \cdots 0e\rangle, |0g0g \cdots 1g\rangle, \dots, |0e0g \cdots 0g\rangle, |1g0g \cdots 0g\rangle\}. \quad (30)$$

In the basis of these states, the Hamiltonian (29) can be represented by a  $2N \times 2N$  matrix. Despite a large size, the matrix can be directly diagonalized and results in  $N$  cell superposition states (eigenstates). We find that among the  $2N$  states, one can distinguish two sets of  $N - 1$  degenerate

antisymmetric eigenstates. These are

$$\begin{aligned} |\phi_1\rangle &= \frac{1}{\mathcal{N}_1} \left[ p_+ |0g0g \cdots 0e\rangle - |0g0g \cdots 1g\rangle + \frac{1}{p_-} |0e0g \cdots 0g\rangle + |1g0g \cdots 0g\rangle \right], \\ |\phi_2\rangle &= \frac{1}{\mathcal{N}_2} [p_+ (|0g0g \cdots 0e\rangle - |0g \cdots 0e0g\rangle) - |0g0g \cdots 1g\rangle + |0g \cdots 1g0g\rangle], \\ &\vdots \\ |\phi_{N-1}\rangle &= \frac{1}{\mathcal{N}_2} [p_+ (|0g0g \cdots 0e\rangle - |0g0e \cdots 0g\rangle) - |0g0g \cdots 1g\rangle + |0g1g \cdots 0g\rangle], \end{aligned} \quad (31)$$

with corresponding eigenenergies

$$\begin{aligned} \omega_1 = z \cdots = \omega_{N-1} \\ = \omega_c - \frac{1}{2}(\Delta - \kappa) + \sqrt{\frac{1}{4}(\Delta - \kappa)^2 + g^2}, \end{aligned} \quad (32)$$

where

$$\begin{aligned} \mathcal{N}_1 = \sqrt{p_+^2 + \frac{1}{p_-^2} + 2}, \quad \mathcal{N}_2 = \sqrt{2p_+^2 + 2}, \\ p_{\pm} = -r \pm \sqrt{r^2 + 1}, \quad r = \frac{\Delta - \kappa}{2g}. \end{aligned} \quad (33)$$

The other set of  $N - 1$  degenerate antisymmetric eigenstates is

$$\begin{aligned} |\phi_N\rangle &= \frac{1}{\mathcal{N}_3} \left[ p_- |0g0g \cdots 0e\rangle - |0g0g \cdots 1g\rangle \right. \\ &\quad \left. + \frac{1}{p_+} |0e0g \cdots 0g\rangle + |1g0g \cdots 0g\rangle \right], \\ |\phi_{N+1}\rangle &= \frac{1}{\mathcal{N}_4} [p_- (|0g0g \cdots 0e\rangle - |0g \cdots 0e0g\rangle) \\ &\quad - |0g0g \cdots 1g\rangle + |0g \cdots 1g0g\rangle], \\ &\vdots \\ |\phi_{2N-2}\rangle &= \frac{1}{\mathcal{N}_4} [p_- (|0g0g \cdots 0e\rangle - |0g0e \cdots 0g\rangle) \\ &\quad - |0g0g \cdots 1g\rangle + |0g1g \cdots 0g\rangle], \end{aligned} \quad (34)$$

with eigenenergies

$$\begin{aligned} \omega_N = \cdots = \omega_{2N-2} \\ = \omega_c - \frac{1}{2}(\Delta - \kappa) - \sqrt{\frac{1}{4}(\Delta - \kappa)^2 + g^2}, \end{aligned} \quad (35)$$

where

$$\mathcal{N}_3 = \sqrt{p_-^2 + \frac{1}{p_+^2} + 2}, \quad \mathcal{N}_4 = \sqrt{2p_-^2 + 2}. \quad (36)$$

The remaining two eigenstates of the system are fully symmetric superposition states,

$$\begin{aligned} |\phi_{\pm}\rangle &= \frac{1}{\mathcal{N}_{\pm}} \left[ \frac{1}{p_{\pm}} (|0g0g \cdots 0e\rangle + |0g0g \cdots 0e0g\rangle + \cdots \right. \\ &\quad \left. + |0e0g \cdots 0g\rangle) + |0g0g \cdots 1g\rangle + |0g0g \cdots 1g0g\rangle \right. \\ &\quad \left. + \cdots + |1g0g \cdots 0g\rangle \right], \end{aligned} \quad (37)$$

with eigenenergies

$$\begin{aligned} \omega_{\pm} = \omega_c - \frac{1}{2}[\Delta + (N - 1)\kappa] \\ \pm \sqrt{\frac{1}{4}[\Delta + (N - 1)\kappa]^2 + g^2}, \end{aligned} \quad (38)$$

respectively, where

$$\mathcal{N}_{\pm} = \sqrt{\frac{N}{p_{\pm}^2} + N}, \quad (39)$$

and

$$p'_{\pm} = -r' \pm \sqrt{r'^2 + 1}, \quad r' = \frac{\Delta + (N - 1)\kappa}{2g}. \quad (40)$$

We note from Eqs. (32), (35), and (38) that for  $g = 0$ , energies of the antisymmetric states cross at  $\Delta = \kappa$ , whereas energies of the two fully symmetric states cross at  $\Delta = -(N - 1)\kappa$ . When  $g \neq 0$ , avoided crossings occur at  $\Delta = \kappa$  for the antisymmetric states, and at  $\Delta = -(N - 1)\kappa$  for the symmetric states. If and only if  $\Delta = -(N - 1)\kappa$  is true, do the eigenstates  $|\phi_{\pm}\rangle$  become  $W$ -type maximally entangled states.

Figure 7 shows the dependence of the energies of the eigenstates  $|\phi_{\pm}\rangle$  on the detuning  $\Delta$ . We see two crossing points when  $g = 0$  and the avoided crossing between the states when  $g \neq 0$ . It clearly illustrates the appearance of two separate groups of degenerate antisymmetric states with the minimum energy separation  $2g$  at  $\Delta = \kappa$ , and two symmetric states with the minimum energy separation  $2g$  at  $\Delta = -(N - 1)\kappa$ .

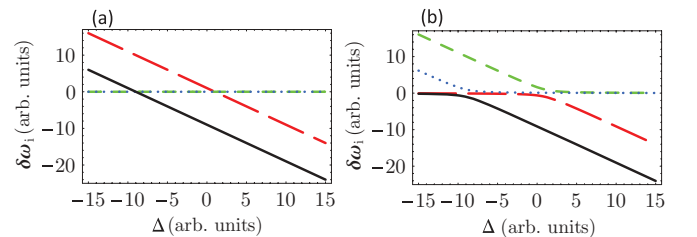


FIG. 7. (Color online) The dependence of the energy difference  $\delta\omega_i = \omega_i - \omega_c$  on the detuning  $\Delta$  (in arbitrary units) of the  $\nu = 1$  eigenstates of  $N = 10$  coupled JC cells for  $\kappa = 1$  and (a)  $g = 0$ , (b)  $g = 1$ . The green short-dashed line is for the set of antisymmetric states  $|\phi_i\rangle$  ( $i = 1, 2, \dots, N - 1$ ), the red long-dashed line is for the set of antisymmetric states  $|\phi_j\rangle$  ( $j = N, N + 1, \dots, 2N - 2$ ), and the blue dotted and black solid lines are for the symmetric states  $|\phi_+\rangle$  and  $|\phi_-\rangle$ , respectively.

Perhaps the most interesting aspects of the  $N$  cell system is that the energies of the antisymmetric states are independent of  $N$ . Adding more cells increases the number of the antisymmetric states but does not affect their energies. Here the antisymmetry is with respect to a permutation of the two entangled JC cells, not of any pair of “qubits,” and it is exact only in the limit of maximal entanglement,  $|p_{\pm}| = 1$ . For the specific case  $N = 2$ , the antisymmetric states  $|\phi_{1,2}\rangle$  correspond to the (subradiant) states  $|+, i\rangle$  introduced in Eq. (16), whereas the symmetric states  $|\phi_{\pm}\rangle$  correspond to the superradiant ones  $|-, i\rangle$ . Note also that  $N = 2$  is the only case in which the antisymmetric and symmetric states have entanglement between the same number of “qubits,” four in this case.

### B. Transition rates

Having derived the explicit forms of the eigenstates  $|\phi_i\rangle$  of the single-excitation sector  $\nu = 1$ , we now turn to calculate transition rates between the eigenstates  $|\phi_i\rangle$  and the ground state  $|0\rangle = |0g \cdots 0g\rangle$ . We consider separately two cases. In the first, we assume that the atoms are coupled to a common reservoir. In the other case, we assume that the atoms are coupled to independent reservoirs.

When the atoms are coupled to a common reservoir, the transitions occur with rates

$$\Gamma_i = \left| \sum_{j=1}^N \sqrt{\gamma_{aj}} \langle \phi_i | \hat{\sigma}_j^\dagger | 0 \rangle \right|^2 + \left| \sum_{j=1}^N \sqrt{\gamma_{cj}} \langle \phi_i | \hat{a}_j^\dagger | 0 \rangle \right|^2. \quad (41)$$

Applying Eqs. (31), (34), and (37), after straightforward calculations we obtain

$$\begin{aligned} \Gamma_1 &= \frac{1}{\mathcal{N}_1^2} \left[ \left( p_+ \sqrt{\gamma_{a1}} + \frac{\sqrt{\gamma_{aN}}}{p_-} \right)^2 + (\sqrt{\gamma_{cN}} - \sqrt{\gamma_{c1}})^2 \right], \\ \Gamma_i &= \frac{1}{\mathcal{N}_2^2} [p_+^2 (\sqrt{\gamma_{a1}} - \sqrt{\gamma_{ai}})^2 + (\sqrt{\gamma_{ci}} - \sqrt{\gamma_{c1}})^2], \\ & \quad i = 2, \dots, N-1, \\ \Gamma_N &= \frac{1}{\mathcal{N}_3^2} \left[ \left( p_- \sqrt{\gamma_{a1}} + \frac{\sqrt{\gamma_{aN}}}{p_+} \right)^2 + (\sqrt{\gamma_{cN}} - \sqrt{\gamma_{c1}})^2 \right], \\ \Gamma_j &= \frac{1}{\mathcal{N}_4^2} [p_-^2 (\sqrt{\gamma_{a1}} - \sqrt{\gamma_{aj}})^2 + (\sqrt{\gamma_{cj}} - \sqrt{\gamma_{c1}})^2], \\ & \quad j = N+1, \dots, 2N-2, \\ \Gamma_{\pm} &= \frac{1}{\mathcal{N}_{\pm}^2} \left[ \frac{1}{p_{\pm}^2} \left( \sum_{i=1}^N \sqrt{\gamma_{ai}} \right)^2 + \left( \sum_{i=1}^N \sqrt{\gamma_{ci}} \right)^2 \right]. \end{aligned} \quad (42)$$

For the case of identical cells,

$$\gamma_{a1} = \cdots = \gamma_{aN} \equiv \gamma_a \quad (43)$$

and

$$\gamma_{c1} = \cdots = \gamma_{cN} \equiv \gamma_c, \quad (44)$$

it follows that the transition rates from all of the antisymmetric states are zero,

$$\Gamma_1 = \cdots = \Gamma_N = \cdots = \Gamma_{2N-2} = 0. \quad (45)$$

Only the fully symmetric states  $|\phi_{\pm}\rangle$  are optically active and are damped at rates

$$\Gamma_{\pm} = \frac{N}{(1 + p_{\pm}^2)} (\gamma_a + p_{\pm}^2 \gamma_c), \quad (46)$$

in which we see the characteristic  $N$  time enhancement, i.e., the superradiant behavior [20,22].

From Eqs. (45) and (46) it is apparent that, just as in the  $N = 2$  case, the  $2N - 2$  antisymmetric states are all optically inactive, whereas the two symmetric ones are superradiant. The distinction is quite convenient because higher-dimensional entanglement is present in the latter states, so a symmetric absorption spectrum would reveal maximal  $2N$ -partite  $W$ -like entanglement shared among all the JC cells.

As the  $N$  cell system radiates only from the fully symmetric states, the Hilbert space of the system is confined to the totally symmetric subspace of two states  $|\phi_{\pm}\rangle$ . Given that there are only two nonzero transition rates from the excited states to the ground state, the absorption spectrum of a weak probe beam monitoring the system is expected to be composed of two peaks. This feature is seen in Fig. 8, which displays the absorption spectrum for coupled  $N = 10$  cells.

As expected, there are two peaks corresponding to transitions from the states  $|\phi_{\pm}\rangle$  to the ground state  $|0\rangle$ . The relative peak amplitudes are a function of  $\Delta$ , and if and only if  $\Delta = -(N - 1)\kappa$ , the amplitudes are equal and symmetrically located about

$$\omega_c - \omega_p = \pm g. \quad (47)$$

When  $\Delta = -(N - 1)\kappa$ , the states  $|\phi_{\pm}\rangle$  reduce to maximally entangled  $W$  states. Hence, a symmetric absorption spectrum is a signature of a maximally entangled  $W$  state with  $2N$  degrees of freedom.

We close this section by evaluating the transition rates for the case when the atoms are damped by independent reservoirs. The total transition rate due to the interaction of the atoms with independent reservoirs and the cavity modes damped by a common reservoir is defined by

$$\Gamma_i = \sum_{j=1}^N \gamma_{aj} |\langle \phi_i | \hat{\sigma}_j^\dagger | 0 \rangle|^2 + \left| \sum_{j=1}^N \sqrt{\gamma_{cj}} \langle \phi_i | \hat{a}_j^\dagger | 0 \rangle \right|^2. \quad (48)$$

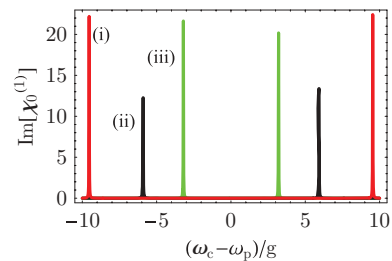


FIG. 8. (Color online) The absorption spectra  $\text{Im}[\chi_0^{(1)}(\omega_p)]$  of coupled  $N = 10$  cells plotted as a function of  $(\omega_c - \omega_p)/g$  for  $\gamma_a/g = 0.05$ ,  $\gamma_c/g = 0.02$ ,  $\kappa/g = 2$ , and different detunings  $\Delta$ :  $\Delta/g = 1$  [green line (iii)],  $\Delta/g = 10$  [black line (ii)], and  $\Delta/g = -18$  [red line (i)].



When we make use of Eqs. (31), (34), and (37) in Eq. (48), we readily obtain

$$\begin{aligned}\Gamma_1 &= \frac{1}{\mathcal{N}_1^2} \left[ \left( p_+^2 \gamma_{a1} + \frac{\gamma_{aN}}{p_-^2} \right) + (\sqrt{\gamma_{cN}} - \sqrt{\gamma_{c1}})^2 \right], \\ \Gamma_i &= \frac{1}{\mathcal{N}_2^2} [p_+^2 (\gamma_{ai} + \gamma_{ai}) + (\sqrt{\gamma_{ci}} - \sqrt{\gamma_{c1}})^2], \\ & i = 2, \dots, N-1, \\ \Gamma_N &= \frac{1}{\mathcal{N}_3^2} \left[ \left( p_-^2 \gamma_{a1} + \frac{\gamma_{aN}}{p_+^2} \right) + (\sqrt{\gamma_{cN}} - \sqrt{\gamma_{c1}})^2 \right], \quad (49) \\ \Gamma_j &= \frac{1}{\mathcal{N}_4^2} [p_-^2 (\gamma_{aj} + \gamma_{aj}) + (\sqrt{\gamma_{cj}} - \sqrt{\gamma_{c1}})^2], \\ & j = N+1, \dots, 2N-2, \\ \Gamma_{\pm} &= \frac{1}{\mathcal{N}_{\pm}^2} \left[ \frac{1}{p_{\pm}^2} \sum_{i=1}^N \gamma_{ai} + \left( \sum_{i=1}^N \sqrt{\gamma_{ci}} \right)^2 \right].\end{aligned}$$

It is easy to see that the transition rates (49) differ significantly from that which we encountered in Eqs. (42) for the decay of the atoms in a common reservoir. Notice that all of the transition rates are now different from zero, and none of the rates can be reduced to zero, indicating no subradiance. This principle also applies to the special case of identical cells,

$$\gamma_{a1} = \dots = \gamma_{aN} \equiv \gamma_a \quad (50)$$

and

$$\gamma_{c1} = \dots = \gamma_{cN} \equiv \gamma_c. \quad (51)$$

However, despite the fact that the transition rates (49) are different from zero, we find that in the case of identical cells and under a strong coupling between the cells ( $\kappa \gg g$ ), the transition rates reduce to

$$\begin{aligned}\Gamma_1 &\approx \gamma_a, \quad \Gamma_i \approx 0, \quad i = 2, \dots, N-1, \\ \Gamma_j &\approx \gamma_a, \quad j = N, \dots, 2N-2, \\ \Gamma_{\pm} &\approx \frac{1}{(1 + p_{\pm}^2)} (\gamma_a + p_{\pm}^2 N \gamma_c).\end{aligned} \quad (52)$$

Clearly, in the limit of a strong coupling, the states  $|\phi_i\rangle$  ( $i = 2, \dots, N-1$ ) do not decay, so they form a decoherence-free subspace. The remaining states decay with nonzero rates. The states  $|\phi_1\rangle, |\phi_N\rangle$ , and  $|\phi_j\rangle$  decay with the rate equal to the single atom decay rate  $\gamma_a$ , whereas the rates  $\Gamma_{\pm}$  show the characteristic  $N$  times enhancement (superradiance), but only with respect to the cavity damping. The contribution to  $\Gamma_{\pm}$  from the atomic part, proportional to  $\gamma_a$ , is independent of  $N$ . This is what one could expect, since the atoms are damped by independent reservoirs. This is also consistent with the results of de Ponte *et al.* [16].

## V. CONCLUSIONS

We have studied a system of coupled Jaynes-Cummings (JC) cells with coupling created by overlapping evanescent cavity fields or by tunneling of photons between the cells. This overlap or tunneling determines the coherent hopping rate between the pair of cavities. This coherent hopping term along with the strength of atom-field coupling within each

cavity determines the unitary dynamics of the closed coupled system. Our analysis also includes incoherent cavity damping and atomic spontaneous emission rates. These incoherent processes are unavoidable in experiments but are sometimes not considered in studies of condensed-matter types of properties of such systems. We included these incoherent terms for completeness and found that ensuring differences in incoherent rates can be quite valuable in detecting entanglement of these coupled atom-cavity systems.

The principal advantages of our treatment are that it allows one to study the relation between the radiative properties of the system and entanglement. For example, in the case of the single JC cell, we have observed that the ratio of the transition rates for the two lowest-doublet states directly reveals the degree of entanglement between the atom and cavity mode provided that the spontaneous emission rate  $\gamma_a$  is not equal to the cavity loss rate  $\gamma_c$ . The degree of entanglement depends on the values of atom-cavity coupling strength  $g$  in the JC Hamiltonian.

We have also studied transition rates from the second doublet to the first doublet for the single JC model. In this case, we have transitions from an entangled  $n = 2$  state to entangled  $n = 1$  states, in contrast to the  $n = 1$  to  $n = 0$  transition from an entangled first-doublet state to a ground state, which is an atom-cavity product state. We have found that the rates depend explicitly on properties of states in both doublets, namely, that it depends explicitly on both  $\theta_n$  and  $\theta_{n-1}$ , but adding the transition rates together as in Eq. (10) only depends on  $\theta_n$ . Thus the transition rates directly reveal the degree of entanglement of the  $n$ th doublet without being mixed up with the degree of entanglement in the lower doublet. Direct measurement of entanglement of the states is possible.

These results on entanglement in the single JC cell are interesting and provide a foundation to study coupled JC cells. For coupled JC cells, we focus only on the  $\nu = 1$  case. We have derived the explicit analytical forms of the transition rates between the  $\nu = 1$  quadruplet of states for the double JC cell to the (product) ground state. There are four rates in this case, and each of these rates conveys information about the degree of entanglement in the state including whether the states are maximally entangled. When loss rates from cells (both spontaneous emission and cavity loss) are equal, information about the degree of entanglement is not obtained by our method but is obtained for unequal rates.

Finally, we have shown how to extend our two JC cell case to an arbitrary number  $N$  of the JC cells such that each cell is coupled to all other cells. We have established conditions for maximal entanglement and calculate the susceptibility. This  $N$ -cell case is likely only of theoretical interest as it is hard to imagine how such a system would be configured in a real experiment, but this general extension to  $N$  cells is interesting nonetheless.

## ACKNOWLEDGMENTS

This work has been supported by NSERC, MITACS, CIFAR, QuantumWorks, iCORE, China's 973 Program No. 2011CB911203 and NSFC Grants No. 11004029 and No. 11174052. B.C.S. is supported by a CIFAR Fellowship.

- [1] E. T. Jaynes and F. W. Cummings, *IEEE Proc.* **51**, 89 (1963).
- [2] H. Paul, *Ann. Phys.* **466**, 411 (1963).
- [3] J. H. Eberly, N. B. Narozhny, and J. J. Sanchez-Mondragon, *Phys. Rev. Lett.* **44**, 1323 (1980).
- [4] H. J. Carmichael, P. Kochan, and B. C. Sanders, *Phys. Rev. Lett.* **77**, 631 (1996); B. C. Sanders, H. J. Carmichael, and B. F. Wielinga, *Phys. Rev. A* **55**, 1358 (1997); M. Brune, F. Schmidt-Kaler, A. Maali, J. Dreyer, E. Hagley, J. M. Raimond, and S. Haroche, *Phys. Rev. Lett.* **76**, 1800 (1996); J. M. Fink, M. Göppl, M. Baur, R. Bianchetti, P. J. Leek, A. Blais, and A. Wallraff, *Nature (London)* **454**, 315 (2008).
- [5] S. J. D. Phoenix and P. L. Knight, *Ann. Phys.* **186**, 381 (1988); J. I. Cirac, P. Zoller, H. J. Kimble, and H. Mabuchi, *Phys. Rev. Lett.* **78**, 3221 (1997).
- [6] M. J. Hartmann, F. Brandão, and M. B. Plenio, *Nature Phys.* **2**, 849 (2006); A. D. Greentree, C. Tahan, J. H. Cole, and L. Hollenberg, *ibid.* **2**, 856 (2006); D. Rossini and R. Fazio, *Phys. Rev. Lett.* **99**, 186401 (2007); D. G. Angelakis, M. F. Santos, and S. Bose, *Phys. Rev. A* **76**, 031805 (2007).
- [7] P. Xue, Z. Ficek, and B. C. Sanders, *Proc. SPIE* **8163**, 81630Q (2011).
- [8] C. Cohen-Tannoudji, J. Dupont-Roc, and G. Grynberg, *Atom-Photon Interactions* (Wiley, New York, 1992).
- [9] R. Kubo, *J. Phys. Soc. Jpn.* **12**, 570 (1957).
- [10] B. R. Mollow, *Phys. Rev. A* **5**, 1522 (1972).
- [11] C. Szymanowski, C. H. Keitel, B. J. Dalton, and P. L. Knight, *J. Mod. Opt.* **42**, 985 (1995).
- [12] R. W. Boyd, M. G. Raymer, P. Narum, and D. J. Harter, *Phys. Rev. A* **24**, 411 (1981).
- [13] M. Skarja, N. M. Borstnik, M. Löffler, and H. Walther, *Phys. Rev. A* **60**, 3229 (1999).
- [14] F. K. Nohama and J. A. Roversi, *J. Mod. Opt.* **54**, 1139 (2007).
- [15] C. D. Ogden, E. K. Irish, and M. S. Kim, *Phys. Rev. A* **78**, 063805 (2008).
- [16] M. A. de Ponte, S. S. Mizrahi, and M. H. Y. Moussa, *Ann. Phys.* **322**, 2077 (2007).
- [17] H. S. Freedhoff, *Phys. Rev. A* **19**, 1132 (1979).
- [18] T. G. Rudolph, Z. Ficek, and B. J. Dalton, *Phys. Rev. A* **52**, 636 (1995).
- [19] H.-P. Breuer and F. Petruccione, *The Theory of Open Quantum Systems* (Oxford University Press, Oxford, 2007).
- [20] R. H. Dicke, *Phys. Rev.* **93**, 99 (1954).
- [21] Z. Ficek and R. Tanaś, *Phys. Rep.* **372**, 369 (2002).
- [22] N. E. Rehler and J. H. Eberly, *Phys. Rev. A* **3**, 1735 (1971).